Half-Integer Quantum Hall Effects and Single Dirac-Cone States in Silicene

Motohiko Ezawa
Department of Applied Physics, University of Tokyo, Hongo 7-3-1, 113-8656, Japan

The massless Dirac electron is expected to display half-integer quantum Hall effect (QHE) at the filling factor $\nu = \pm 1/2, \pm 3/2, \pm 5/2, \cdots$, reflecting the parity anomaly. However, it has so far been unable to materialize such a series due to the fermion doubling problem inherent to the chiral symmetric lattice system. For instance, the QHE in graphene displays a series $\nu = \pm 2, \pm 6, \pm 10, \cdots$ because of the 4-fold degeneracy of each Landau level. We demonstrate that the half-integer series $\nu = \pm 1/2, \pm 3/2, \pm 5/2, \cdots$ can arise in silicene, which is a silicon cousin of graphene, when we break the chiral, time-reversal and inversion symmetries all together by applying electric field and photo-irradiation simultaneously. A prominent hallmark is the emergence of a single Dirac-cone (SDC) state, which contains one massless Dirac cone and three massive Dirac cones in the Brillouin zone. A SDC state is a topologically protected semimetal since it emerges along the boundary between two distinctive topological insulators. The half-integer QHE is predicted to appear in such a SDC state.

The study of graphene has begun with the experimental discovery of an unconventional quantum Hall effect (QHE) with Hall plateaux at the filling factor $\nu = \pm 2, \pm 6, \pm 10, \cdots$[1, 2], implying the 4-fold degeneracy of each Landau level. The Hall conductivity increases by e^2/h when the Fermi energy crosses one Landau level. If there were no degeneracy the Hall conductivity would be half-integer quantized[3],

$$\sigma_{\rm H} = \pm(n+1/2)e^2/h, \quad n = 0, 1, 2, \cdots . \tag{1}$$

It reflects the parity anomaly of the massless Dirac fermion[4, 5]. This is also a result of the particle-hole symmetry together with the fact that the Landau level of the massless Dirac fermion resides at exactly zero energy[6]. However the "half integer" is hidden in graphene under the 4-fold degeneracy associated with the spin and valley degrees of freedom. Though there is a long history in quest for the genuine half-integer QHE given by (1), it has never been discovered. This is because the necessary condition is the emergence of a single massless Dirac-cone state, which we call a single Dirac-cone (SDC) state for brevity. The main obstacle is the Nielsen-Ninomiya theorem, which requires an even number of massless Dirac fermions in the chiral symmetric lattice system[7]. In the surface of the topological insulator, a SDC state is realized because two Dirac cones are split into the top and bottom surfaces[8, 9]. However, this resolution is only superficial: In a slab geometry electrons on the top and bottom surfaces contribute to the Hall conductance all together, yielding the integer QHE[10].

Silicene[11–13, 17, 23] may well open a way to materialize the genuine half-integer series (1). Silicene consists of a honeycomb lattice of silicon atoms with buckled sublattices made of A sites and B sites. The states near the Fermi energy are π orbitals residing near the K and K' points at opposite corners of the hexagonal Brillouin zone. The low-energy dynamics in the K and K' valleys is described by the Dirac theory as in graphene, but electrons are massive due to a relatively large spin-orbit (SO) coupling. Silicene is a quantum spin Hall (QSH) insulator[14], which is a particular type of a two-dimensional topological insulator.

The Kane-Mele model[14, 15] describes well silicene. In addition, a staggered potential and the Haldane term[16] may be introduced to the system by applying external electric field[17] and a circularly polarized photo-irradiation[18, 19], respectively. A rich topological phase diagram is obtained since the electric field breaks the space inversion symmetry and the photo-irradiation breaks the time-reversal symmetry. Furthermore, the mass term breaks the chiral symmetry, invalidating the Nielsen-Ninomiya theorem in the system. We are thus able to create a SDC state[19], which contains one massless Dirac cone and three massive Dirac cones [Fig.1]. In this paper we analyze the QHE. We demonstrate that, by tuning the electric field and the photo-irradiation, the massless electron leads to the half-integer QHE given by (1). The other three masses are different, and the plateaux series is predicted to be $\pm 1/2, \pm, 3/2, \pm 5/2, \cdots$.

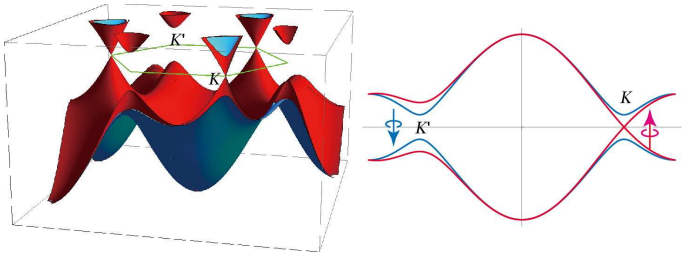

FIG. 1: Illustration of a SDC state, which consists one massless Dirac cone and three masive Dirac cones in the valence band. In this instance, up-spin (red) electrons are massless at the K point but massive at the K' point, while down-spin (blue) electrons are massive both at the K and K' points.

We analyze the Kane-Mele-Haldane Hamiltonian in the presence of the staggered sublattice potential term. The tight-binding model is[15, 17, 19],

$$H = -t \sum_{\langle i,j\rangle\alpha} c^\dagger_{i\alpha} c_{j\alpha} + i\frac{\lambda_{\rm SO}}{3\sqrt{3}} \sum_{\langle\langle i,j\rangle\rangle\alpha\beta} \nu_{ij} c^\dagger_{i\alpha} \sigma^z_{\alpha\beta} c_{j\beta} + i\frac{\lambda_\Omega}{3\sqrt{3}} \sum_{\langle\langle i,j\rangle\rangle\alpha\beta} \nu_{ij} c^\dagger_{i\alpha} c_{j\beta} + \ell \sum_{i\alpha} \mu_i E_z c^\dagger_{i\alpha} c_{i\alpha}, \tag{2}$$

where $c^\dagger_{i\alpha}$ creates an electron with spin polarization α at site i, and $\langle i,j\rangle$ / $\langle\langle i,j\rangle\rangle$ run over all the nearest/next-nearest neighbor hopping sites. We explain each term. (i) The first term

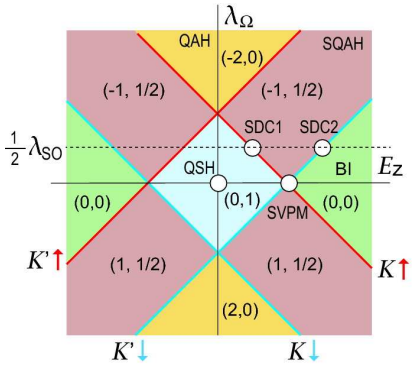

FIG. 2: Phase diagram in the (E_z, λ_Ω) plane. A circle shows a point where the Dirac-cone structure is given in Fig.3. Heavy lines represent phase boundaries indexed by K_η and s_z =↑↓. There appear a SDC state along the line, which is characterized by a single gapless Dirac cone at the K_η point with spin s_z. The topological charges (C, C_s) are indicated. We give the band gaps along the holizontal lines at $\lambda_\Omega = 0$ and $\lambda_\Omega = \lambda_{\mathrm{SO}}/2$ (dotted line) in Fig.3.

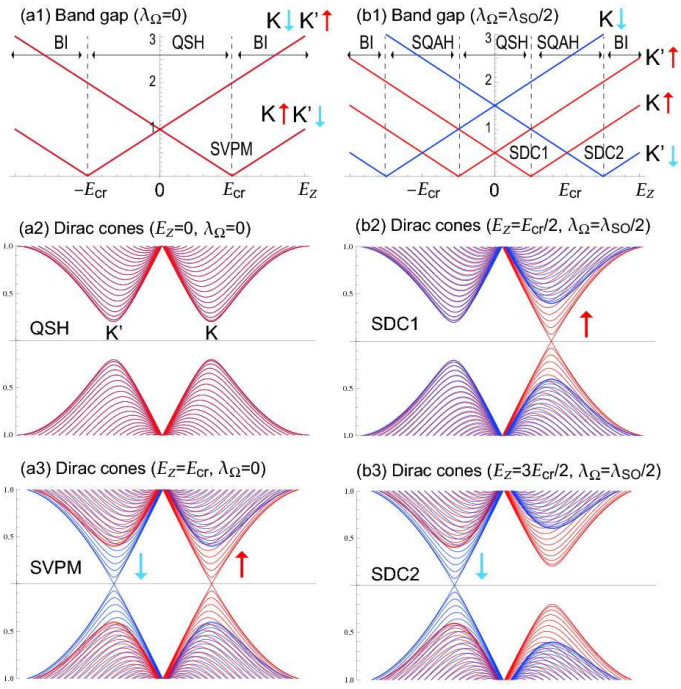

FIG. 3: (a1,b1) The band gaps as a function of E_z with the fixed values of $\lambda_\Omega = 0$ and $\lambda_\Omega = \frac{1}{2}\lambda_{\mathrm{SO}}$. (a2,a3,b2,b3) The structure of four Dirac cones at special points as indicated by circles in Fig.2. (a2) The band gap is open in the QSH insulator. (a3) There are two massless Dirac cones in the SVPM state. (b2,b3) These are typical SDC states. We have set $\lambda_{\mathrm{SO}} = 0.2t$ for illustration.

represents the usual nearest-neighbor hopping with the transfer energy $t = 1.6$eV. (ii) The second term[15, 20] represents the effective SO coupling with $\lambda_{\mathrm{SO}} = 3.9$meV, where $\boldsymbol{\sigma} = (\sigma_x, \sigma_y, \sigma_z)$ is the Pauli matrix of spin, with $\nu_{ij} = +1$ if the next-nearest-neighboring hopping is anticlockwise and $\nu_{ij} = -1$ if it is clockwise with respect to the positive z axis. (iii) The third term represents the Haldane interaction induced by the photo-irradiation, where $\lambda_\Omega = \hbar v_{\mathrm{F}}^2 \mathcal{A}^2 \Omega^{-1}$ with Ω the frequency and $\mathcal{A}$ the dimensionless intensity[18, 19]. (iv) The fourth term[17] is the staggered sublattice potential term. Due to the buckled structure the two sublattice planes are separated by a distance, which we denote by 2ℓ with $\ell = 0.23$Å. It generates a staggered sublattice potential $\propto 2\ell E_z$ between silicon atoms at A sites and B sites in electric field E_z.

The low-energy effective Dirac Hamiltonian in the momentum space reads[15, 17, 19]

$$H_\eta = \hbar v_{\mathrm{F}} \left(\eta k_x \tau_x + k_y \tau_y\right) + \lambda_{\mathrm{SO}} \sigma_z \eta \tau_z - \ell E_z \tau_z + \lambda_\Omega \eta \tau_z, \tag{3}$$

where $v_{\mathrm{F}} = \frac{\sqrt{3}}{2} at = 5.5 \times 10^5$m/s is the Fermi velocity with the lattice constant $a = 3.86$Å, and $\boldsymbol{\tau} = (\tau_x, \tau_y, \tau_z)$ is the Pauli matrix of the sublattice pseudospin. The factor $\eta = \pm 1$ distinguishes the K and K' points.

The Hamiltonian (3) describes a four-component Dirac fermion indexed by the spin $s_z = \pm 1$ and the valley $\eta = \pm 1$. We use s_z =↑↓ and η =K,K' for indices to make their meaning clear. The coefficient of τ_z is summarized as $\Delta_{s_z}^\eta$. It is the mass of the Dirac electron with the spin s_z in the valley η,

$$\Delta_{s_z}^\eta = \eta s_z \lambda_{\mathrm{SO}} - \ell E_z + \eta \lambda_\Omega, \tag{4}$$

which may be positive, negative or zero. The band gap is given by $2|\Delta_{s_z}^\eta|$. It is a remarkable feature that we can control the spin-valley dependent mass $\Delta_{s_z}^\eta$ by changing the electric field E_z and the photo-irradiation strength λ_Ω.

Silicene is an ideal playground to explore topological insulators and topological phase transitions[8, 9]. The topological quantum numbers are the Chern number $\mathcal{C}$ and the $\mathbb{Z}_2$ index. When the spin s_z is a good quantum number, as is the case of the present model, the $\mathbb{Z}_2$ index is identical to the spin-Chern number $\mathcal{C}_s$ modulo 2. They are defined by $\mathcal{C} = \mathcal{C}_\uparrow^{\mathrm{K}} + \mathcal{C}_\uparrow^{\mathrm{K'}} + \mathcal{C}_\downarrow^{\mathrm{K}} + \mathcal{C}_\downarrow^{\mathrm{K'}}$ and $\mathcal{C}_s = \frac{1}{2}(\mathcal{C}_\uparrow^{\mathrm{K}} + \mathcal{C}_\uparrow^{\mathrm{K'}} - \mathcal{C}_\downarrow^{\mathrm{K}} - \mathcal{C}_\downarrow^{\mathrm{K'}})$, where $\mathcal{C}_{s_z}^\eta$ is the summation of the Berry curvature in the momentum space over all occupied states of electrons with spin s_z in the Dirac valley η. It is straightforward to calculate $\Delta_{s_z}^\eta$, which are given by[8, 9, 21]

$$\mathcal{C}_{s_z}^\eta = \frac{\eta}{2} \mathrm{sgn}(\Delta_{s_z}^\eta) \tag{5}$$

as a function of the Dirac mass $\Delta_{s_z}^\eta$.

It is a trivial task to derive the topological phase diagram in the (E_z, λ_Ω) plane, just by calculating the topological numbers $(\mathcal{C}, \mathcal{C}_s)$ with the help of (5), as illustrated in Fig.2. A topological phase transition occurs when the sign of the mass changes. There are four phase boundaries [Fig.2], which are given by solving $\Delta_{s_z}^\eta = 0$, corresponding to s_z =↑↓ and η =K,K'. Let us review two typical cases.

We increase E_z from $E_z = 0$ while keeping $\lambda_\Omega = 0$ in the phase diagram [Fig.2]. We show the band gap $2|\Delta_{s_z}^\eta|$ as a function of E_z in Fig.3(a1). The Dirac cones at $E_z = 0$ are illustrated in Fig.3(a2). As E_z increases, two Dirac masses decrease and vanishes ($\Delta_\uparrow^{\mathrm{K}} = \Delta_\downarrow^{\mathrm{K'}} = 0$) at $E_z = E_{\mathrm{cr}}$ as in Fig.3(a1). Silicene becomes a spin-valley polarized semimetal (SVPM), where the Dirac cones are illustrated in Fig.3(a3).

Doubling of massless fermions occurs. As E_z increases further, the gap opens again and silicene becomes a trivial bund insulator (BI) [Fig.2].

We next increase E_z while keeping $\lambda_\Omega = \lambda_{\rm SO}/2$ in the phase diagram [Fig.2]. Two Dirac masses ($\Delta^{\rm K}_\uparrow$ and $\Delta^{\rm K'}_\downarrow$) decrease and the other two ($\Delta^{\rm K}_\downarrow$ and $\Delta^{\rm K'}_\uparrow$) increase, as illustrated in 3(b1). We find $\Delta^{\rm K}_\uparrow = 0$ at $E_z = \frac{1}{2}E_{\rm cr}$, where up-spin electrons are massless at the K point while all others are massive, as the Dirac cones show in 3(b2). This is a SDC state (SDC1). As E_z increases further, the gap opens again and silicene becomes a spin-polarized quantum anomalous Hall (SQAH) insulator. We also find $\Delta^{\rm K'}_\downarrow = 0$ at $E_z = \frac{3}{2}E_{\rm cr}$, where down-spin electrons are massless at the K' point while all others are massive, as the Dirac cones show in Fig.3(b3). This is another SDC state (SDC2).

We proceed to apply a homogeneous magnetic field $\boldsymbol{B} = \boldsymbol{\nabla}\times\boldsymbol{A} = (0,0,-B)$ with $B>0$ along the z axis to silicene. The Hamiltonian is given by making the minimal substitution, $\hbar k_i \to P_i \equiv \hbar k_i + eA_i$, in the Hamiltonian (3). We introduce a pair of Landau-level ladder operators,

$$\hat{a} = \frac{\ell_B(P_x + iP_y)}{\sqrt{2}\hbar}, \quad \hat{a}^\dagger = \frac{\ell_B(P_x - iP_y)}{\sqrt{2}\hbar}, \tag{6}$$

satisfying $[\hat{a},\hat{a}^\dagger] = 1$, where $\ell_B = \sqrt{\hbar/eB}$ is the magnetic length. The Hamiltonian H_η is block diagonal and given by

$$H_\eta = \begin{pmatrix} H^\eta_\uparrow & 0 \\ 0 & H^\eta_\downarrow \end{pmatrix}, \tag{7}$$

with the diagonal elements being

$$H^{\rm K}_{s_z} = \begin{pmatrix} \Delta^{\rm K}_{s_z}(E_z) & \hbar\omega_{\rm c}\hat{a}^\dagger \\ \hbar\omega_{\rm c}\hat{a} & -\Delta^{\rm K}_{s_z}(E_z) \end{pmatrix}, \tag{8}$$

$$H^{\rm K'}_{s_z} = \begin{pmatrix} \Delta^{\rm K'}_{s_z}(E_z) & -\hbar\omega_{\rm c}\hat{a} \\ -\hbar\omega_{\rm c}\hat{a}^\dagger & -\Delta^{\rm K'}_{s_z}(E_z) \end{pmatrix} \tag{9}$$

in the basis $\{\psi_A,\psi_B\}^t$.

It is straightforward to solve the eigen equation of $H^\eta_{s_z}$. The lowest Landau level is special, where the eigenvalue is

$$E^\eta_{s_z} = \eta\Delta^\eta_{s_z}(E_z). \tag{10}$$

The eigenstate describes electrons when $E^\eta_{s_z} > 0$ and holes when $E^\eta_{s_z} < 0$. For higher Landau levels they are given by

$$\pm E_N = \pm\sqrt{(\hbar\omega_c)^2 N + (\Delta^\eta_{s_z})^2}, \quad N = 1,2,\cdots, \tag{11}$$

where $\pm$ for the electron and hole states.

The present result is applicable also to the QHE in graphene by setting the Dirac mass zero for all spin-valley components ($\Delta^\eta_{s_z} = 0$). We have the 4-fold degeneracy in all Landau levels. Provided the electron-hole symmetry is required, the series reads $\nu = \pm 2, \pm 6, \pm 10, \cdots$, as is consistent with the experimental fact[1, 2].

We next consider silicene without electric field ($E_z = E_{\rm cr}$) and photo-irradiation ($\lambda_\Omega = 0$), where the Dirac mass reads

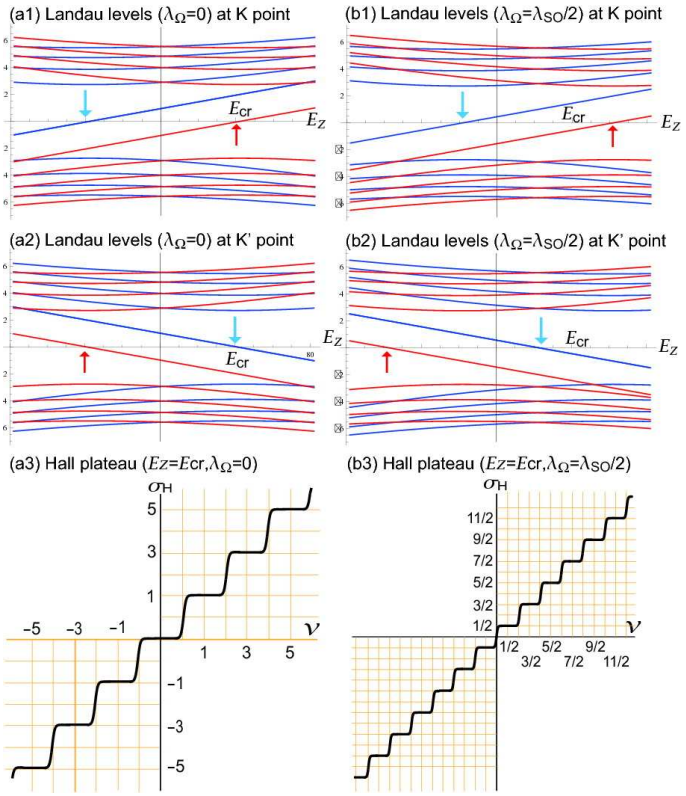

FIG. 4: (a1,a2,b1,b2) Landau levels as a function of E_z at special points of $\lambda_\Omega = 0, \frac{1}{2}\lambda_{\rm SO}$. The two lines crossing the E_z-axis represent the lowest Landau levels. (a1,a2) The lowest Landau level resides at exactly zero energy for $E_z = \pm E_{\rm cr}$ when $\lambda_\Omega = 0$. All levels are doubly degenerate. (a3) Hall plateaux develop at $\nu = \pm 1, \pm 3, \pm 5, \cdots$. (b1,b2) The lowest Landau level resides at exactly zero energy for $E_z = \pm\frac{1}{2}E_{\rm cr}, \pm\frac{3}{2}E_{\rm cr}$ when $\lambda_\Omega = \frac{1}{2}\lambda_{\rm SO}$. All levels are nondegenerate. (b3) Hall plateaux develop at $\nu = \pm 1/2, \pm 3/3, \pm 5/5, \cdots$. We have set $\lambda_{\rm SO} = 0.2t$ for illustration.

$\Delta^\eta_{s_z} = \eta s_z \lambda_{\rm SO}$. Each levels are doubly degenerate, and hence the series reads[22] $\nu = \pm 1, \pm 3, \pm 5, \cdots$.

Finally we analyze the SDC state at $E_z = \frac{1}{2}E_{\rm cr}$ and $\lambda_\Omega = \lambda_{\rm SO}$, where only electrons with $s_z = \uparrow$ at the K point are massless. All levels are nondegenerate, and the series read $\nu = \pm 1/2, \pm 3/3, \pm 5/5, \cdots$, by requiring the electron-hole symmetry. There are many other SDC states along the phase boundary [Fig.2], where the half-integer QHE (1) appears.

In conclusion, we have investigated the Kane-Mele-Haldane Hamiltonian in the presence of the staggered sublattice potential term. SDC states emerge along the phase boundaries in the phase diagram [Fig.2]. The SDC state contains one massless Dirac cone and three massive Dirac cones. Such a state is allowed because we break the chiral, time-reversal and inversion symmetries explicitly. We have demonstrated the occurrence of half-integer QHE in the SDC state.

The model (3) describes well silicene under electric field and photo-irradiation. There are actually small correction terms due to Rashba interactions[19]. However we can numerically show[22] that these terms produce quantitatively

minor corrections and not change our conclusions. Furthermore we can make the following arguments on this point.

In general, when the topological numbers change across the boundary, the band must close and yield gapless modes in the interface. Otherwise the topological numbers cannot change the values across the interface. Now, a SDC state appears along the boundary between two distinctive topological insulators. Since they are topologically protected, the SDC state is also topologically protected against small perturbations. Consequently, we may say that the SDC state is a topological semimetal.

One might question the validity of the electron-hole symmetry when higher order corrections are included into the model. Even so, we wish to emphasize that the QHE is a phenomenon taking place in the vicinity of half-filling, where the Dirac system (3) describes the system very well and the electron-hole symmetry is a good symmetry. Indeed, the experimetal observation of the unconventional QHE at $\nu = \pm 2, \pm 6, \pm 10, \cdots$ in graphene[1, 2] supports this conclusion because higher order corrections are common to graphene and silicene.

I am very much grateful to N. Nagaosa and Y. Hatsugai for many fruitful discussions on the subject. This work was supported in part by Grants-in-Aid for Scientific Research from the Ministry of Education, Science, Sports and Culture No. 22740196.

[1] K. S. Novoselov, A. K. Geim, S. V. Morozov, D. Jiang, M. I. Katsnelson, I. V. Grigorieva, S. V. Dubonos, and A. A. Firsov, Nature 438, 360 (2005).
[2] Y. Zhang, Y. W. Tan, H. L. Stormer and P. Kim, Nature 438, 201 (2005).
[3] Y. Zheng and T. Ando, Phys. Rev. B 65, 245420 (2002).
[4] A. N. Redlich, Phys. Rev. D 29, 2366 (1984).
[5] G. W. Semenoff, Phys. Rev. Lett. 53, 2449 (1984).
[6] R. Jackiw, Phys. Rev. D 29, 2375 (1984).
[7] H.B. Nielsen, M. Ninomiya, Nucl.Phys. B 185 20 (1981).
[8] M.Z Hasan and C. Kane, Rev. Mod. Phys. **82**, 3045 (2010).
[9] X.-L. Qi and S.-C. Zhang, Rev. Mod. Phys. **83**, 1057 (2011).
[10] L. Fu and C. L. Kane, Phys. Rev. B 76, 045302 (2007).
[11] P. Vogt, , P. De Padova, C. Quaresima, J. A., E. Frantzeskakis, M. C. Asensio, A. Resta, B. Ealet and G. L. Lay, Phys. Rev. Lett. **108**, 155501 (2012).
[12] C.-L. Lin, R. Arafune, K. Kawahara, N. Tsukahara, E. Minamitani, Y. Kim, N. Takagi, M. Kawai, Appl. Phys. Express 5, Art No. 045802 (2012) .
[13] A. Fleurence, R. Friedlein, T. Ozaki, H. Kawai, Y. Wang, and Y. Yamada-Takamura, Phys. Rev. Lett. **108**, 245501 (2012).
[14] C.-C. Liu, W. Feng, and Y. Yao, Phys. Rev. Lett. **107**, 076802 (2011).
[15] C.-C. Liu, H. Jiang, and Y. Yao, Phys. Rev. B, **84**, 195430 (2011).
[16] F. D. M. Haldane, Phys. Rev. Lett. 61, 2015 (1988).
[17] M. Ezawa, New J. Phys. 14, 033003 (2012).
[18] T. Kitagawa, T. Oka, A. Brataas, L. Fu, and E. Demler, Phys. Rev. B 84, 235108 (2011).
[19] M. Ezawa, Phys. Rev. Lett. 110, 026603 (2013).
[20] C. L. Kane and E. J. Mele, Phys. Rev. Lett. **95**, 226801 (2005).
[21] M. Ezawa, Eur. Phys. J. B 85, 363 (2012).
[22] M. Ezawa, J. Phys. Soc. of Jpn 81, 064705 (2012).
[23] M. Ezawa, Phys. Rev. Lett 109, 055502 (2012).